

## Static equation of state of bcc iron

H. L. Zhang,<sup>1</sup> S. Lu,<sup>1</sup> M. P. J. Punkkinen,<sup>1,2,\*</sup> Q.-M. Hu,<sup>1,3</sup> B. Johansson,<sup>1,4</sup> and L. Vitos<sup>1,4,5</sup>

<sup>1</sup>*Applied Materials Physics, Department of Materials Science and Engineering, Royal Institute of Technology, SE-10044 Stockholm, Sweden*

<sup>2</sup>*Department of Physics and Astronomy, University of Turku, FIN-20014 Turku, Finland*

<sup>3</sup>*Shenyang National Laboratory for Materials Sciences, Institute of Metal Research, Chinese Academy of Sciences, 72 Wenhua Road, Shenyang 110016, China*

<sup>4</sup>*Division of Materials Theory, Department of Physics and Materials Science, Uppsala University, P.O. Box 530, SE-75121 Uppsala, Sweden*

<sup>5</sup>*Research Institute for Solid State Physics and Optics, P.O. Box 49, H-1525 Budapest, Hungary*

(Received 25 May 2010; revised manuscript received 10 September 2010; published 28 October 2010)

Body-centered-cubic (bcc) iron is one of the most investigated solid-state systems. Using four different density-functional methods, we show that there is a magnetic transition close to the ground-state volume of bcc Fe, which originates from the particular magnetic band structure. The common equation of state functions, used to determine the basic ground-state physical quantities from the calculated total energies, cannot capture the physics of this magnetic transition leading to serious underestimation of the Fe bulk modulus. Ignorance of the magnetic transition found here is reflected by large scatter of the published theoretical bulk moduli of ferromagnetic bcc Fe. Due to the low performance of the exchange-correlation functionals, most of the erroneous results are accidentally in good agreement with the experimental values. The present finding is of fundamental importance, especially taking into account that bcc Fe is frequently used as a test system in assessing the performance of exchange-correlation approximations or total-energy methods.

DOI: [10.1103/PhysRevB.82.132409](https://doi.org/10.1103/PhysRevB.82.132409)

PACS number(s): 75.50.Bb, 64.30.Ef, 71.15.Mb, 71.15.Nc

The exact form of the exchange-correlation (XC) density functional is not known. The most common approximation, the local-density approximation, has been remarkably successful in many applications, but fails for some systems, e.g., transition metals and transition-metal oxides. Significantly better agreement between experiment and theory for the basic ground-state properties of transition metals was achieved by introducing gradient corrections, which led to the generalized gradient approximation (GGA) (Refs. 1–6) or to the subsystem functional.<sup>7–11</sup> However, it is still difficult to describe all kinds of solids satisfactorily with a particular exchange-correlation functional.<sup>12–14</sup> Therefore, alternative functionals are continuously designed and taken into use. It is very important to test the accuracy of these approximations by using well-established test systems. The same applies also when assessing the performance of newly developed electronic-structure methods.

The bcc iron ( $\alpha$ -Fe) is one of the most severe test systems.<sup>12,15–19</sup> This is due to the enormous significance of Fe in numerous technological applications, but also to the challenges related to magnetism and open 3d electronic shell. The most basic physical quantities considered when assessing the performance of an *ab initio* approach are the ground-state volume [described here by the equilibrium Wigner-Seitz radius ( $R_{\text{WS}}$ )] and bulk modulus ( $B$ ). The ground-state properties of ferromagnetic bcc Fe have been investigated by different groups using various first-principles methods. A few representative results are listed in Table I for two common density-functional approximations: Perdew-Wang-91 (PW91) (Ref. 3) and Perdew-Burke-Ernzerhof (PBE).<sup>4</sup> The theoretical  $R_{\text{WS}}$  are basically close to each other. The agreement with the experimental equilibrium radii is also satisfactory, although it is well known that both GGA functionals underestimate slightly the ground-state volume of Fe. However, it is interesting that the bulk moduli from

different authors scatter significantly (from 144 to about 215 GPa, in comparison with the experimental values from about 160 to about 170 GPa), even when the same computational tool and exchange-correlation approximation was adopted.

In this Brief Report, we investigate the static equation of state of ferromagnetic bcc Fe using four different first-principles methods. We show that the inconsistency of the bulk moduli from different calculations originates from a volume-induced magnetic transition taking place at about 2% lattice expansion.

The four employed density-functional methods are the exact muffin-tin orbitals (EMTO) method,<sup>17,56</sup> the projector augmented wave method<sup>18,57</sup> as implemented in Vienna *ab initio* simulation package<sup>58–61</sup> (VASP), a pseudopotential method<sup>62</sup> (CASTEP), and the augmented plane-wave plus local orbitals method<sup>63</sup> (WIEN2K). Below we briefly describe the most important numerical details for each of these tools. Calculations were carried out within the scalar-relativistic approach and employed the PBE generalized gradient approximation for the exchange-correlation functional.<sup>4</sup> In EMTO calculations, we used *spdf* basis set and  $29 \times 29 \times 29$  uniformly distributed  $k$  points in the irreducible Brillouin zone. The self-consistent calculations were performed within the soft-core approximation and the total energy was obtained from the self-consistent charge density using the full charge-density technique<sup>17,64</sup> In VASP, CASTEP, and WIEN2K calculations, Brillouin zone sampling was performed by the Monkhorst-Pack scheme.<sup>65</sup> In VASP, the chosen plane-wave cut-off energy (700 eV) and  $k$  mesh ( $49 \times 49 \times 49$   $k$  points) lead to convergence in total energy within 0.1 meV per atom. The CASTEP calculations were run through the Accelrys Materials Studio Modeling 4.2 interface by using the ultrasoft pseudopotential. The same cut-off energy and  $k$  mesh were used to sample the Brillouin zone as in VASP. In WIEN2K calculations, the plane-wave cut-off energy was 306

TABLE I. Equilibrium Wigner-Seitz radius ( $R_{WS}$ , in Bohr's radius  $a_B$ ) and bulk modulus ( $B$ , in GPa) of ferromagnetic bcc Fe from theoretical and experimental data. The different gradient-corrected XC's are the PBE (Ref. 4) and PW91 (Refs. 3 and 6). Details about the employed theoretical tools can be found in the corresponding references.

	Method	XC	$R_{WS}$ ( $a_B$ )	$B$ (GPa)
Theory	FLAPW	PBE	2.634 (Ref. 20), 2.634 (Ref. 21), 2.635 (Ref. 22),	186 (Ref. 20), 194 (Ref. 21), 200 (Ref. 22), 186 (Ref. 23),
			2.643 (Ref. 23), 2.652 (Ref. 24), 2.636 (Ref. 16)	188 (Ref. 24), 198 (Ref. 16)
	FLAPW	PW91	2.630 (Ref. 25), 2.637 (Ref. 26), 2.642 (Ref. 27),	186 (Ref. 25), 189 (Ref. 26), 174 (Ref. 27), 172 (Ref. 28),
			2.662 (Ref. 28), 2.660 (Ref. 29)	169 (Ref. 29)
	PAW	PBE	2.634 (Ref. 15)	185 (Ref. 15)
	PAW	PW91	2.631 (Ref. 30), 2.634 (Ref. 31), 2.641 (Ref. 32),	194 (Ref. 30), 174 (Ref. 31), 172 (Ref. 32), 174 (Ref. 18),
			2.634 (Ref. 18), 2.671 (Ref. 33)	176 (Ref. 33)
	US-PP	PW91	2.657 (Ref. 34), 2.650 (Ref. 35), 2.653 (Ref. 18)	160 (Ref. 34), 176 (Ref. 35), 151 (Ref. 18)
	US-PP	PBE	2.699 (Ref. 36)	144 (Ref. 36)
	US-AE	PW91	2.634 (Ref. 18)	175 (Ref. 18)
	FPKKR	PW91	2.630 (Ref. 25), 2.645 (Ref. 37)	188 (Ref. 25), 184 (Ref. 37)
	MEAM	PW91	2.665 (Ref. 38)	173 (Ref. 38)
	LMTO	PW91	2.639 (Ref. 39), 2.689 (Ref. 40)	176 (Ref. 39), 215 (Ref. 40)
	FPLMTO	PBE	2.617 (Ref. 41)	201 (Ref. 41)
EMTO	PBE	2.640 (Ref. 42)	194 (Ref. 42)	
Expt.			2.668 (Ref. 43), 2.668 (Ref. 44), 2.666 (Ref. 45),	173 (Ref. 43), 167 (Ref. 44), 169 (Ref. 45), 172 (Ref. 46),
			2.661 (Ref. 46), 2.671 (Ref. 47), 2.662 (Ref. 48),	168 (Ref. 47), 170 (Ref. 48), 172 (Ref. 49), 172 (Ref. 50),
			2.667 (Ref. 49), 2.667 (Ref. 50), 2.671 (Ref. 51),	168 (Ref. 51), 159 (Ref. 52), 170 (Ref. 53), 166 (Ref. 54),
			2.666 (Ref. 52), 2.670 (Ref. 53), 2.669 (Ref. 54),	172 (Ref. 55)
			2.662 (Ref. 55)	

eV and the Brillouin zone was sampled by  $28 \times 28 \times 28$   $k$ -point mesh. The muffin-tin radius was set to 2.0 Bohr's radius ( $a_B$ ). The EMTO, VASP, CASTEP, and WIEN2K total energies were computed for atomic radii  $R=2.50a_B-2.80a_B$  with an interval of  $0.01a_B$ .

The  $R_{WS}$  and  $B$  are usually determined by fitting the calculated total energies to some equation of state function. The Murnaghan, Morse, and Birch-Murnaghan (B-M) forms are the most commonly used fitting functions.<sup>66-70</sup> It is well known that the bulk modulus is very sensitive to the data used and to the employed equation of state. In our study, all three mentioned fitting functions have been used to evaluate the  $R_{WS}$  and  $B$  of ferromagnetic bcc Fe. It was found that the B-M function is the best and most adjusting function of these fitting functions as it leads to the smallest scatter of the bulk modulus for different fitting intervals. Therefore, in Table II we present  $R_{WS}$ ,  $B$ , and the standard deviation ( $\sigma$ ) from the B-M fitting for different sets of data points in Table II.

For all four first-principles methods adopted here, the equilibrium  $R_{WS}$  and  $B$  remain almost constant when using the data points between  $R=2.50a_B-2.65a_B$  and  $R=2.50a_B-2.70a_B$ . Namely, using the fitting interval below  $2.70a_B$  generates the smallest equilibrium  $R_{WS}$ , largest  $B$ , and smallest standard deviation  $\sigma$ . When we include the energy points beyond  $2.70a_B$  (fitting intervals  $R=2.50a_B-2.75a_B$  and  $R=2.50a_B-2.80a_B$ ) we find that  $R_{WS}$  increases slightly but  $B$  decreases significantly. The marked increase of  $\sigma$  indicates that the fitting quality becomes worse when the energies calculated for  $R \geq 2.70a_B$  are also included. We ascribe the pronounced change in the bulk modulus of ferromagnetic bcc Fe to a volume-induced magnetic transition near  $2.70a_B$ .

In order to understand the above data-set-dependent equation of state of bcc Fe, we investigated the magnetic moment of ferromagnetic bcc Fe as a function of the volume (Fig. 1, left axis). It is noted that there is a well-distinguished jump in the magnetic moment around  $2.7a_B$ . Such a jump influences the total energy and makes the data points with  $R > 2.7a_B$  deviate from the equation of state determined by the rest of the data points ( $R < 2.7a_B$ ). In Fig. 1 (right axis) the calculated (VASP-PBE) total energies are shown along with the B-M fits for intervals  $2.5a_B-2.7a_B$  and  $2.5a_B-2.8a_B$ . The fit on the data points between  $2.5a_B-2.7a_B$  reproduces rather well the calculated total energies. However, the fit including all points between  $2.5a_B-2.8a_B$  clearly underestimates the total energies at both low (around  $2.55a_B$ ) and high (around  $2.7a_B$ ) volumes, resulting in a reduced bulk modulus as compared to the first fit function. Fixed spin calculations were also performed within the  $2.7a_B-2.8a_B$  interval using the estimated moments obtained by extrapolating linearly the magnetic moments from the interval  $R=2.60a_B-2.68a_B$ . These additional results (not shown) indicate that indeed the sudden increase in the magnetic moment significantly affects total energy. Finally, we note that similar calculations were carried out using the Ceperley-Alder<sup>71</sup> LDA functional parametrized by Perdew and Zunger<sup>72</sup> and the PW91 (Refs. 3 and 6) GGA functional. These results demonstrate that the same phenomenon is found also by other exchange-correlation functionals but the suitable energy range for fitting depends slightly on the employed functional.

The implication of our findings is that, due to the magnetic transition around  $R=2.7a_B$ , the total energies should be fitted using the values obtained for volumes smaller than this

TABLE II. Equilibrium Wigner-Seitz radius ( $R_{WS}$ , in  $a_B$ ), bulk modulus ( $B$ , in GPa), and standard deviation ( $\sigma$ ) for ferromagnetic bcc Fe obtained by the theoretical tools (EMTO, VASP, WIEN2K, and CASTEP). The equation of state was determined using the Birch-Murnaghan fitting function for data points calculated between  $2.50a_B-2.65a_B$ ,  $2.50a_B-2.70a_B$ ,  $2.50a_B-2.75a_B$ , and  $2.50a_B-2.80a_B$ , respectively.

Method	2.50–2.65	2.50–2.70	2.50–2.75	2.50–2.80
	$R_{WS}$			
EMTO	2.640	2.640	2.643	2.645
VASP	2.642	2.642	2.644	2.646
WIEN2K	2.636	2.635	2.636	2.638
CASTEP	2.618	2.618	2.620	2.621
	$B$			
EMTO	190.72	189.67	179.84	171.37
VASP	187.03	187.48	179.91	171.91
WIEN2K	192.46	193.78	188.99	179.78
CASTEP	213.42	212.98	200.18	191.67
	$\sigma$			
EMTO	0.000009	0.000012	0.000142	0.000213
VASP	0.000009	0.000009	0.000117	0.000192
WIEN2K	0.000011	0.000014	0.000084	0.000202
CASTEP	0.000017	0.000028	0.000173	0.000232

critical value. This is because the commonly used fitting functions cannot capture the above magnetic transition. It is important to realize that the improved agreement between the experiment and theory for  $B$  when including the larger volumes is only accidental. This can simply be understood by considering the equilibrium volume. The calculated  $R_{WS}$  for bcc Fe (static conditions) is slightly smaller than the experimental  $R_{WS}$ . Therefore, one would expect slightly larger

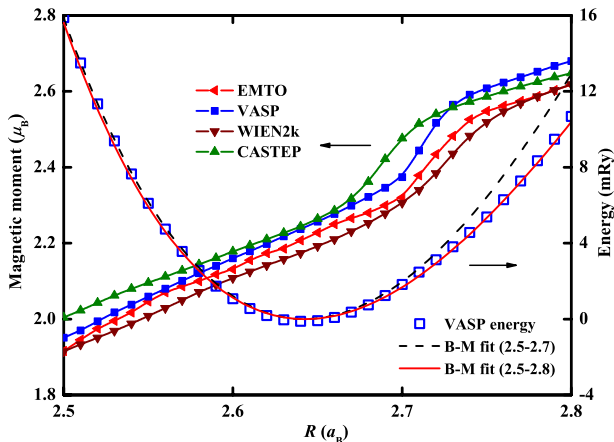


FIG. 1. (Color online) Magnetic moment per atom (in  $\mu_B$ , solid symbols connected with solid lines, left axis) and total energy (in mRy, open squares, right axis) of ferromagnetic bcc Fe as a function of the atomic radius  $R$  (in  $a_B$ ). The magnetic moments were obtained by the EMTO, VASP, WIEN2K, and CASTEP methods and the total energy by the VASP method. The corresponding B-M fits are shown for the intervals  $2.5a_B-2.7a_B$  (black dashed line) and  $2.5a_B-2.8a_B$  (red solid line).

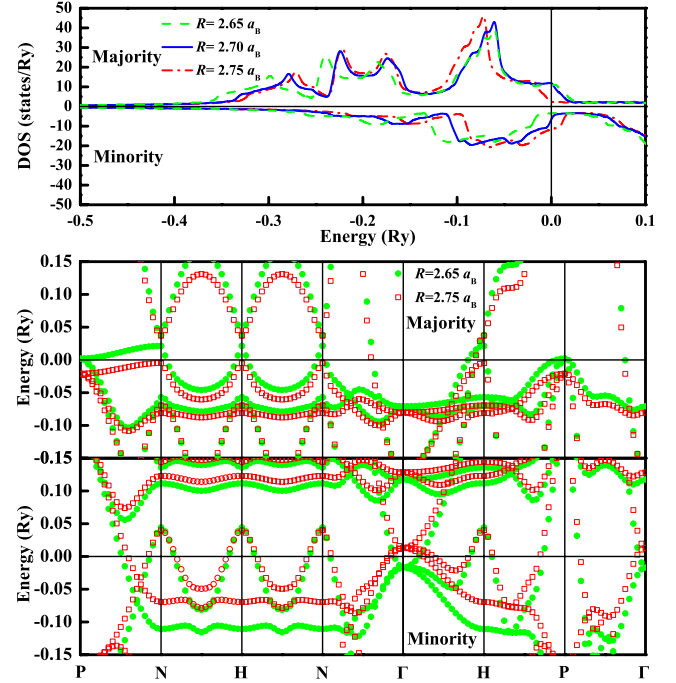


FIG. 2. (Color online) Upper panel: theoretical (VASP) spin-resolved DOS of ferromagnetic bcc Fe at three different volumes,  $R=2.65a_B$  (green dashed line),  $R=2.70a_B$  (blue solid line), and  $R=2.75a_B$  (red dashed-dotted line). Lower panel: band structure of the majority and minority spin channels for  $R=2.65a_B$  (green solid circles) and  $R=2.75a_B$  (red open squares).

$B$  compared to the experiment, which is indeed the case, if  $B$  is calculated properly by considering only the volumes below the magnetic transition.

An explanation for the observed magnetic transition can be found in the electronic structure of bcc Fe by monitoring the density of states (DOS) around the Fermi energy ( $E_F$ ). Figure 2 (upper panel) shows the spin-resolved DOS for the ferromagnetic bcc Fe for  $R=2.65a_B$ ,  $2.70a_B$ , and  $2.75a_B$ . With increasing volume the exchange splitting increases, shifting the Fermi level toward larger (smaller) energies within the majority (minority) bands. Indeed, one can see that around  $R=2.7a_B$ ,  $E_F$  hits the bottom of the pseudogap in the minority DOS [ $N^\downarrow(E)$ ] and reaches the shoulder of the majority DOS [ $N^\uparrow(E)$ ]. Therefore, by increasing the radius beyond  $\sim 2.7a_B$ ,  $N^\downarrow(E_F)$  rapidly increases resulting in decreasing occupation in the minority channel. At the same time,  $N^\uparrow(E_F)$  experiences a drop from shoulder to bottom, which is accompanied by a small increase in the majority occupation number. The combined effects lead to a sudden increase in the magnetic moment, in line with Fig. 1. A detailed analysis of the band structures of bcc Fe indicates<sup>73</sup> that the above transitions occur in the minority  $T_{2g}$  band near the  $\Gamma$  point and majority  $T_{2g}$  band near the P point. The calculated (VASP-PBE) energy bands are shown for the high-symmetry  $k$  directions in Fig. 2 (lower panel). As the volume increases the width of the valence band decreases due to decreased interatomic interaction, which leads to the occupation of the minority spin band near the  $\Gamma$  point and deoccupation of the majority spin band near the P point at  $E_F$ .

We have shown that the choice of the fitting interval

affects strongly the calculated bulk modulus of bcc Fe, which is in this respect more sensitive quantity than the volume. This is due to the magnetic transition found around  $R=2.7a_B$ . Such magnetic transition is explained by the spin-resolved density of states specific to ferromagnetic bcc Fe. Our finding explains the large scatter found in the values of  $B$  in literature and has remarkable implications concerning, e.g., the test use of the bcc Fe. The better agreement obtained between the experimental and theoretical bulk moduli by including the volumes above the volume of the magnetic tran-

sition onset is artificial and erroneous and reflects the inaccuracies of the best-performing exchange-correlation energy functionals for Fe and other  $3d$  transition metals.

The Swedish Research Council, the Swedish Foundation for Strategic Research, the Swedish Energy Agency, the Swedish Iron Office (Jernkontoret), the Carl Tryggers Foundation, and the China Scholarship Council are acknowledged for financial support. Part of the calculations was performed using the facilities of the Finnish IT Center for Science.

\*Corresponding author; marpunk@utu.fi

- <sup>1</sup>J. P. Perdew and W. Yue, *Phys. Rev. B* **33**, 8800 (1986).
- <sup>2</sup>J. P. Perdew, *Phys. Rev. B* **33**, 8822 (1986).
- <sup>3</sup>J. P. Perdew, *Electronic Structure of Solids '91* (Akademie Verlag, Berlin, 1991).
- <sup>4</sup>J. P. Perdew *et al.*, *Phys. Rev. Lett.* **77**, 3865 (1996).
- <sup>5</sup>J. P. Perdew *et al.*, *Phys. Rev. Lett.* **100**, 136406 (2008).
- <sup>6</sup>J. P. Perdew *et al.*, *Phys. Rev. B* **46**, 6671 (1992).
- <sup>7</sup>W. Kohn and A. E. Mattsson, *Phys. Rev. Lett.* **81**, 3487 (1998).
- <sup>8</sup>L. Vitos *et al.*, *Phys. Rev. B* **62**, 10046 (2000).
- <sup>9</sup>L. Vitos *et al.*, *Phys. Rev. A* **61**, 052511 (2000).
- <sup>10</sup>R. Armiento and A. E. Mattsson, *Phys. Rev. B* **66**, 165117 (2002).
- <sup>11</sup>R. Armiento and A. E. Mattsson, *Phys. Rev. B* **72**, 085108 (2005).
- <sup>12</sup>M. Ropo *et al.*, *Phys. Rev. B* **77**, 195445 (2008).
- <sup>13</sup>G. I. Csonka *et al.*, *Phys. Rev. B* **79**, 155107 (2009).
- <sup>14</sup>P. Haas *et al.*, *Phys. Rev. B* **80**, 195109 (2009).
- <sup>15</sup>A. E. Mattsson and R. Armiento, *Phys. Rev. B* **79**, 155101 (2009).
- <sup>16</sup>S. Kurth *et al.*, *Int. J. Quantum Chem.* **75**, 889 (1999).
- <sup>17</sup>L. Vitos, *Phys. Rev. B* **64**, 014107 (2001).
- <sup>18</sup>G. Kresse and D. Joubert, *Phys. Rev. B* **59**, 1758 (1999).
- <sup>19</sup>E. G. Moroni *et al.*, *Phys. Rev. B* **56**, 15629 (1997).
- <sup>20</sup>R. Iglesias and S. L. Palacios, *Acta Mater.* **55**, 5123 (2007).
- <sup>21</sup>F. Tran *et al.*, *Phys. Rev. B* **75**, 115131 (2007).
- <sup>22</sup>A. Zupan *et al.*, *Phys. Rev. B* **58**, 11266 (1998).
- <sup>23</sup>G. Y. Guo and H. H. Wang, *Chin. J. Phys.* **38**, 949 (2000).
- <sup>24</sup>H. Ma *et al.*, *Phys. Rev. B* **66**, 024113 (2002).
- <sup>25</sup>M. Asato *et al.*, *Phys. Rev. B* **60**, 5202 (1999).
- <sup>26</sup>L. Stixrude *et al.*, *Phys. Rev. B* **50**, 6442 (1994).
- <sup>27</sup>H. C. Herper *et al.*, *Phys. Rev. B* **60**, 3839 (1999).
- <sup>28</sup>Z. Tang *et al.*, *Phys. Rev. B* **65**, 195108 (2002).
- <sup>29</sup>J.-H. Cho and M. Scheffler, *Phys. Rev. B* **53**, 10685 (1996).
- <sup>30</sup>J. Z. Liu *et al.*, *Phys. Rev. B* **72**, 144109 (2005).
- <sup>31</sup>D. E. Jiang and E. A. Carter, *Phys. Rev. B* **67**, 214103 (2003).
- <sup>32</sup>K. J. Caspersen *et al.*, *Phys. Rev. Lett.* **93**, 115501 (2004).
- <sup>33</sup>L. T. Kong and B. X. Liu, *J. Alloys Compd.* **414**, 36 (2006).
- <sup>34</sup>C. Domain and C. S. Becquart, *Phys. Rev. B* **65**, 024103 (2001).
- <sup>35</sup>L. Vočadlo *et al.*, *Faraday Discuss.* **106**, 205 (1997).
- <sup>36</sup>U. V. Waghmare *et al.*, *Comput. Phys. Commun.* **137**, 341 (2001).
- <sup>37</sup>R. Zeller *et al.*, *Philos. Mag. B* **78**, 417 (1998).
- <sup>38</sup>B.-J. Lee *et al.*, *Phys. Rev. B* **64**, 184102 (2001).
- <sup>39</sup>C. Amador *et al.*, *Phys. Rev. B* **46**, 1870 (1992).
- <sup>40</sup>M. Körling and J. Häglund, *Phys. Rev. B* **45**, 13293 (1992).
- <sup>41</sup>X. Sha and R. E. Cohen, *Phys. Rev. B* **74**, 214111 (2006).
- <sup>42</sup>H. L. Zhang *et al.*, *Phys. Rev. B* **79**, 224201 (2009).
- <sup>43</sup>J. A. Rayne and B. S. Chandrasekhar, *Phys. Rev.* **122**, 1714 (1961).
- <sup>44</sup>C. A. Rotter and C. S. Smith, *J. Phys. Chem. Solids* **27**, 267 (1966).
- <sup>45</sup>J. Leese and A. E. Lord, Jr., *J. Appl. Phys.* **39**, 3986 (1968).
- <sup>46</sup>G. Simmons and H. Wang, *Single Crystal Elastic Constants and Calculated Aggregate Properties* (MIT Press, Cambridge, MA, 1971).
- <sup>47</sup>D. J. Dever, *J. Appl. Phys.* **43**, 3293 (1972).
- <sup>48</sup>V. L. Moruzzi *et al.*, *Calculated Electronic Properties of Metals* (Pergamon, New York, 1978).
- <sup>49</sup>A. P. Jephcoat *et al.*, *J. Geophys. Res.* **91**, 4677 (1986).
- <sup>50</sup>G. Ghosh and G. B. Olson, *Acta Mater.* **50**, 2655 (2002).
- <sup>51</sup>C. Kittel, *Introduction to Solid State Physics*, 7th ed. (Wiley, New York, 1996).
- <sup>52</sup>S. Klotz and M. Braden, *Phys. Rev. Lett.* **85**, 3209 (2000).
- <sup>53</sup>J. J. Adams *et al.*, *J. Appl. Phys.* **100**, 113530 (2006).
- <sup>54</sup>G. R. Speich *et al.*, *Metall. Trans.* **3**, 2031 (1972).
- <sup>55</sup>M. Acet *et al.*, *Phys. Rev. B* **49**, 6012 (1994).
- <sup>56</sup>L. Vitos, in *Computational Quantum Mechanics for Materials Engineers* (Springer-Verlag, London, 2007).
- <sup>57</sup>P. E. Blöchl, *Phys. Rev. B* **50**, 17953 (1994).
- <sup>58</sup>G. Kresse and J. Furthmüller, *Comput. Mater. Sci.* **6**, 15 (1996).
- <sup>59</sup>G. Kresse and J. Furthmüller, *Phys. Rev. B* **54**, 11169 (1996).
- <sup>60</sup>G. Kresse and J. Hafner, *Phys. Rev. B* **47**, 558 (1993).
- <sup>61</sup>G. Kresse and J. Hafner, *Phys. Rev. B* **49**, 14251 (1994).
- <sup>62</sup>S. J. Clark *et al.*, *Z. Kristallogr.* **220**, 567 (2005).
- <sup>63</sup>P. Blaha *et al.*, *WIEN2k, An Augmented Plane Wave+Local Orbitals Program for Calculating Crystal Properties* (TU Vienna, Austria, 2009).
- <sup>64</sup>J. Kollár *et al.*, *Electronic Structure and Physical Properties of Solids: The Uses of the LMTO Method*, Lectures Notes in Physics (Springer-Verlag, Berlin, 2000).
- <sup>65</sup>H. J. Monkhorst and J. D. Pack, *Phys. Rev. B* **13**, 5188 (1976).
- <sup>66</sup>F. D. Murnaghan, *Proc. Natl. Acad. Sci. U.S.A.* **30**, 244 (1944).
- <sup>67</sup>C. L. Fu and K. M. Ho, *Phys. Rev. B* **28**, 5480 (1983).
- <sup>68</sup>V. L. Moruzzi *et al.*, *Phys. Rev. B* **37**, 790 (1988).
- <sup>69</sup>F. Birch, *Phys. Rev.* **71**, 809 (1947).
- <sup>70</sup>A. R. Oganov and P. I. Dorogokupets, *Phys. Rev. B* **67**, 224110 (2003).
- <sup>71</sup>D. M. Ceperley and B. J. Alder, *Phys. Rev. Lett.* **45**, 566 (1980).
- <sup>72</sup>J. P. Perdew and A. Zunger, *Phys. Rev. B* **23**, 5048 (1981).
- <sup>73</sup>H. L. Zhang *et al.*, *Phys. Rev. B* **81**, 184105 (2010).